Vertical multiple-slot waveguide ring resonators in silicon nitride

Laurent Vivien[1,*], Delphine Marris-Morini[1], Amadeu Griol[2], Kristinn B. Gylfason[3], Daniel Hill[2], Jesús Álvarez[2], Hans Sohlström[3] Juan Hurtado[2], David Bouville[1] and Eric Cassan[1]

[1] *Institut d'Electronique Fondamentale, CNRS UMR 8622, Bât. 220, Université Paris-Sud 11, F-91405 ORSAY cedex – France*
[2] *Nanophotonics Technology Center, Universidad Politécnica de Valencia, Camino de Vera s/n, Valencia, Spain*
[3] *Microsystem Technology Laboratory, School of Electrical Engineering, KTH – Royal Institute of Technology, Osquldas väg 10, SE-10044 Stockholm, Sweden*
[*]*Corresponding author: Laurent.vivien@u-psud.fr*

Abstract: This article describes the first demonstration of ring resonators based on vertical multiple-slot silicon nitride waveguides. The design, fabrication and measurement of multiple-slot waveguide ring resonators with several coupling distances and ring radii (70 µm, 90 µm and 110 µm) have been carried out for TE and TM polarizations at the wavelength of 1.3 µm. Quality factors of 6,100 and 16,000 have been achieved for TE and TM polarization, respectively.

©2008 Optical Society of America

OCIS codes: (230.7370) Waveguides; (230.0230) Optical devices; (070.5753) Resonators; (130.0130) Integrated optics; (130.3120) Integrated optics devices.

References and links

1. S. Lardenois, D. Pascal, L. Vivien, E. Cassan, S. Laval, R. Orobtchouk, M. Heitzmann, N. Bouaida, and L. Mollard," Low-loss sub-micrometer SOI rib waveguides and corner mirrors," Opt. Lett. **28**, 1150-1152 (2003).
2. P. Dumon, W. Bogaerts, V. Wiaux, J. Wouters, S. Beckx, J. Van Campenhout, D. Taillaert, B. Luyssaert, P. Bienstman, D. Van Thourhout, and R. Baets, "Low-loss SOI photonic wires and ring resonators fabricated with deep UV lithography," IEEE Photon. Technol. Lett **16**, 1328-1330 (2004).
3. V. Almeida, Q. Xu, C.A. Barrios, and M. Lipson, "Guiding and confining light in void nanostructure," opt. Lett. **29**, 1209-1211 (2004)
4. T. Baehr-Jones, M. Hochberg, C. Walker, and Scherer, "High-Q optical resonators in silicon-on-insulator-based slot waveguides," Appl. Phys. Lett. **86**, 081101 (2005).
5. H. G. Yoo, Y. Fu, D. Riley, J. H. Shin, and P. M. Fauchet, "Birefringence and optical power confinement in horizontal multi-slot waveguides made of Si and SiO2," Opt. Express **16**, 8623-8628 (2008).
6. R. Sun, P. Dong, N-N. Feng, C-Y Hong, J. Michel, M. Lipson, and L. Kimerling, "Horizontal single and multiple slot waveguides : optical transmission at λ=1550nm," Opt. Express **15**, 17967-17972 (2007).
7. C. A. Barrios, B. Sànchez, K. B. Gylfason, A. Griol, H. Sohlström, M. Holgado, and R. Casquet, "Demonstration of slot-waveguide structures on silicon nitride/silicon oxide platform," Opt. Express **15**, 6846-6857 (2007).
8. C. A. Barrios, M. J. Bañuls, V. Gonzàlez-Pedro, K. B. Gylfason, B. Sànchez, A. Griol, A. Maquieira, H. Sohlström, M. Holgado, and R. Casquet, "Label-free optical biosensing with slot-waveguides," Opt. Lett. **33**, 708-710 (2008).
9. U. Levy, M. Abashin, K. Ikeda, A. Krishnamoorthy, J. Cunningham, and Y. Fainman, "Inhomogenous Dielectric Metamaterials with Space-Variant Polarizability," Phys. Rev. Lett. **98**, 243.901 (2007).
10. S-H Yang, M. L. Cooper, P. R. Bandaru, and S. Mookherjea, "Giant birefringence in multi-slotted silicon nanophotonic waveguides," Opt. Express **16**, 8306-8316 (2008).
11. X. Tu, X Xu, S. Chen, J. Yu, and Q. Wang, "Simulation demonstration and experimental fabrication of multiple-slot waveguide," IEEE Phot. Techn. Lett. **20**, 333-335 (2008).
12. PhotonDesign: URL: www.photonDesign.com
13. A. Yariv, "Universal relations for coupling of optical power between microresonators and dielectric waveguides," Electron. Lett. **36**, 321-322 (2000).

1. Introduction

In rib [1] and strip [2] waveguides, light is predominantly guided in the high index material. The light thus has little interaction with the surrounding medium. This is a drawback for biosensing applications where small index variations of the surrounding medium are monitored. Slot waveguides present an interesting alternative [3]. In such a waveguide, light is confined in a low index slot region sandwiched between two high index rails. Due to the discontinuity of the electric field at the interface between the rails and slot, a significant fraction of the electromagnetic field is localized in the slot.

Thanks to the high index contrast of the silicon/silicon oxide system, it has been extensively applied to highly integrated optical circuits and high Q-factor resonators have been obtained [4]. However, for silicon slot waveguides operating in the near infrared the slot needs to be narrower than 100 nm which makes fabrication difficult. A way to meet the fabrication constraints and to reduce propagation loss, is to use horizontal slot waveguides [5,6]. Alternatively, one can relax the fabrication tolerances by using silicon nitride instead of silicon to reduce the refractive index contrast. In this configuration, the slot can be enlarged up to 200 nm [7] which furthermore facilitates sample transport inside the slot for biosensing applications [8]. Recently, vertical multiple-slot structures have been studied [9-11]. In a multiple-slot structure, further enhancement of the optical confinement in the low index slot regions is possible [6,10,11].

In this paper, we experimentally demonstrate the first vertical multiple-slot waveguide using a silicon nitride / silicon oxide platform at a wavelength of about 1.3 μm for both quasi-TE and quasi-TM light polarizations.

2. Design and fabrication

A schematic cross-sectional view of the studied multiple-slot waveguide is depicted in Fig. 1(a). It consists of a silicon substrate, a silicon oxide bottom cladding layer, a 300 nm thick silicon nitride layer, and a silicon oxide top cladding layer. A triple slot structure is chosen for this study.
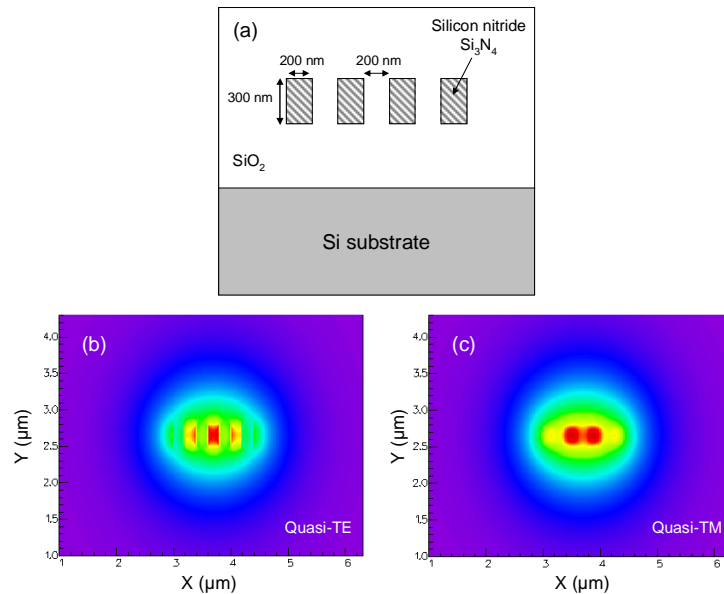

Fig. 1. (a) A schematic cross-section of the multiple-slot waveguide surrounded by silicon oxide top and bottom claddings. The slot and rail widths are both 200 nm and the silicon nitride waveguide height is 300 nm. (b) Calculated electric field distribution of the quasi-TE mode (E_x) and (c) of the quasi-TM mode (H_x) at a wavelength of 1.3 μm. The refractive indices of silicon nitride and silicon oxide are 2.00 and 1.45, respectively.

First, simulations were done to find waveguide dimensions yielding single mode propagation at a wavelength of 1.3 µm for both quasi-TE and quasi-TM polarizations. Fixing the rail height at 300 nm, this condition is obtained for slot and rail widths of 200 nm. All simulations have been carried out using the film mode matching method (FMM) [11]. Figure 1(b) and 1(c) report the electric and magnetic fields of TE and TM polarizations, respectively. We notice that for the TE polarization, the E_x field is confined in the low index slot regions. While for the TM mode, the H_x field is localized in the middle of the multiple-slot waveguide and mainly in the high index material.

The fraction of the optical mode power flux that propagates in the 3 slots (not including other parts of the cladding) is estimated to be about 18 % and 14% for TE and TM polarizations, respectively. In comparison, for a vertical single slot waveguide this fraction is only 11% and 6.5% for TE and TM polarizations, respectively. Higher fractions are achievable by using materials with greater index contrast. For single slot waveguides in silicon/silicon oxide, power fractions of 30% have been reported [3], but applying our fraction definition yields, 22% is obtained for that particular structure. A power fraction of 56% was reported for a triple slot silicon/silicon oxide waveguide [6].

For sensing applications, one aims for a large effective index variation for a small refractive index variation of the top cladding. Figure 2 presents the normalized effective index variation ($\Delta n_{eff}/n_{eff}$) as a function of the top cladding-layer refractive index changes (Δn_{clad}) for the three 300nm high structures: (i) a 900nm wide strip waveguide, (ii) a single-slot waveguide [7] and (iii) the multiple-slot waveguide.
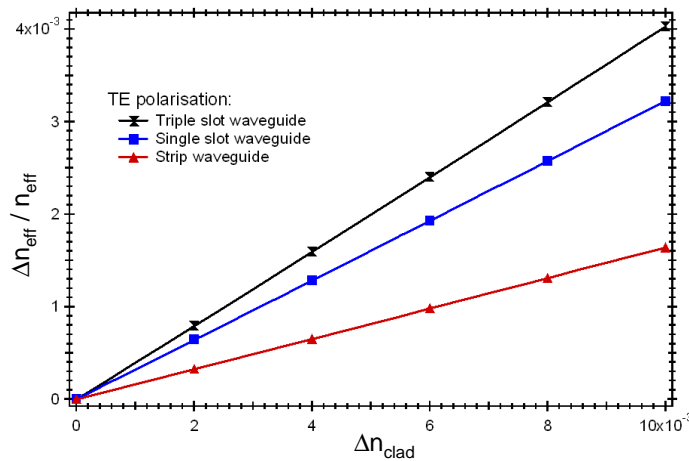

Fig. 2. A comparison of the effective index change as a function of the variation of the refractive index of the top cladding (from 1.45 to 1.46) at a wavelength of 1.3 µm for a 900 nm wide strip waveguide, a single-slot waveguide and the multiple-slot waveguide. Refractive indices of silica and silicon nitride are 1.45 and 1.95, respectively.

One notices an improvement of the effective index variation using multiple-slot waveguide of about 20% and 60% in comparison with single slot waveguide and strip waveguide, respectively. This clearly demonstrates the suitability of the multiple-slot structure for sensing purposes.

The waveguides were fabricated using the following process: First, a 5 µm thick bottom silicon oxide cladding was thermally grown at 1100°C on a 4" silicon wafer. A 300 nm thick silicon nitride film was then deposited by low pressure chemical vapor deposition (LPCVD) at 800°C from NH_3 and SiH_2Cl_2 precursors. A hard mask was patterned by electron beam lithography of PMMA (Raith 150 system), followed by chromium evaporation and lift-off. The waveguide pattern was then transferred to the nitride layer by dry etching in a He/CF_4 plasma. Finally, the guides were covered by a 1 µm thick silicon dioxide top cladding by

TEOS LPCVD at 720°C. Based on previous work with single slot waveguides of the same aspect ratio [7], we expect a small void in the top cladding filling at the top of the slot.

The radius R of the ring resonators is varied from 70 µm to 110 µm and several gaps d are tested. Scanning electron microcope (SEM) images of a ring resonator based on multiple-slot waveguides is shown in fig. 3(b) and 3(c).
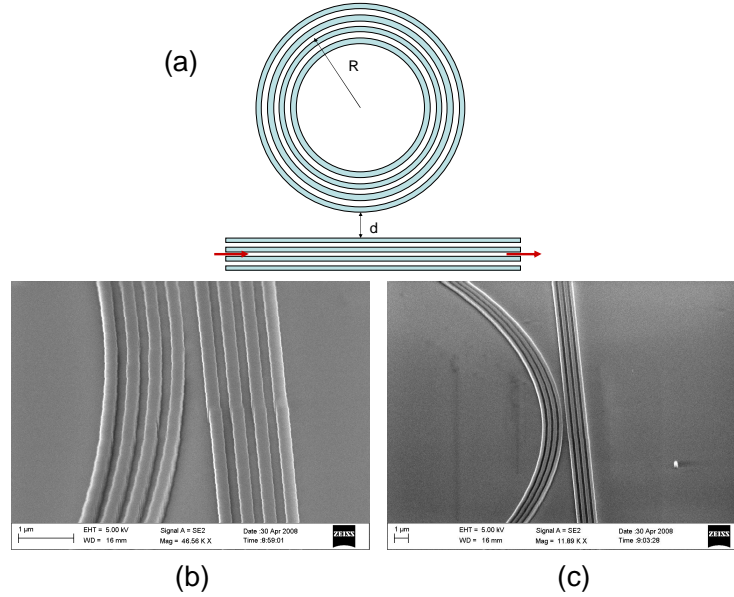

Fig. 3. (a) A schematic top view of the ring resonator based on multiple-slot waveguides. (b) and (c) Scanning electron microscope (SEM) images of a silicon nitride multiple-slot waveguide ring resonator before silicon oxide top cladding deposition.

3. Results and discussion

The ring resonators were characterized using a tunable laser (Tunics Plus) at a wavelength of 1.3 µm. A linearly polarized light beam was coupled into the input waveguide using a polarization maintaining lensed optical fiber. Light was then recorded by a photodiode as a function of the wavelength for both polarizations. Figure 4(a) and (c) show the transmission spectra from 1240 nm to 1340 nm for both TE and TM polarizations of a 90 µm radius multiple-slot waveguide ring resonator. Figure 4(b) and 3(d) report the normalized transmission of one of the resonances for both TE and TM polarizations at a wavelength of about 1250 nm. The gap d is 500 nm. The extinctions at resonance are larger than 6 dB and about 10 dB for the TE and TM polarizations, respectively.

The free spectral ranges (FSR) and the measured group indices ($n_g(\lambda)$) given by Eq. (1) at around 1275 nm are summarized in Tab. 1.

$$n_g(\lambda) \approx \frac{\lambda_0{}^2}{2\pi \cdot (FSR) \cdot R} \tag{1}$$

The obtained group indices vary from 1.613 to 1.633 for TE polarization and vary from 1.623 to 1637 for TM polarization. The simulated group indices obtained using FMM method [12] and taking into account the curvature of the waveguide are 1.616 and 1.631 for TE and TM polarizations, respectively. The simulations show no meaningful variation of the group index for the three radii considered. One notices for both TE and TM polarizations, a good agreement between experimental and theoretical group indices that indicates a well concordance between simulated and fabricated structures.

Resonators are also characterized by their quality factor, which is given by Eq. (2):

$$Q = \frac{\lambda_0}{\Delta\lambda_{-3dB}},$$
(2)

where $\Delta\lambda_{-3dB}$ is the full bandwidth at half maximum of the dropped power and λ_0 is the resonance wavelength.
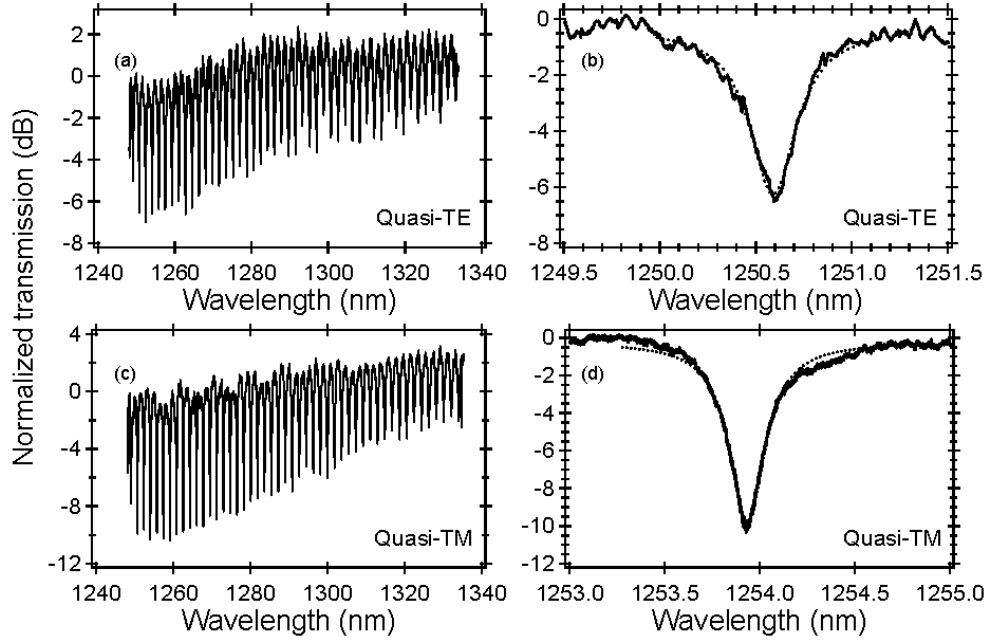

Fig. 4. Measured normalized transmission (solid line) of a 90 µm radius multiple-slot waveguide ring resonator for quasi-TE (a, b) and quasi-TM (c, d) polarizations. The dashed line (b, d) presents the Lorentzian fitting for both polarizations. The gap d is 500 nm.

The optical power transmitted (I_t) through the bus waveguide is given by [13]:

$$I_t = I_0 \frac{a^2 + t^2 - 2\,a\,t\,cos(\phi)}{1 + a^2\,t^2 - 2\,a\,t\,cos(\phi)}$$
(3)

where I_0 is the incident optical power, t the field transmission coefficient, $\phi = \frac{2\pi\,n_{eff}\,(2\pi R)}{\lambda}$ the phase shift for a roundtrip along the resonator, n_{eff} the effective index of the guided mode, $a = e^{-\alpha_r \pi R}$ the attenuation of the field for a roundtrip and α_r the loss coefficient of the ring waveguide.

Table 1. The mean FSR and the measured group indices around 1275 nm of multiple-slot ring resonators with 70 µm, 90 µm, and 110 µm radii. The estimated uncertainty of group index is of 0.2.

		FSR (nm)	Measured group index
R = 70 µm	TE	-	-
	TM	2.277±0.006	1.62±0.2
R = 90 µm	TE	1.782±0.006	1.61±0.2
	TM	1.756±0.006	1.64±0.2
R = 110 µm	TE	1.440±0.006	1.63±0.2
	TM	1.443±0.006	1.63±0.2

For TE-polarization, the maximum measured Q-factors, determined by Eq. 1, are 6,100 for a 90 µm radius ring resonator with a gap of 400 nm and 6,300 for a 110 µm radius resonators with a gap of 500 nm. For TM-polarization, the measured Q-factors reach ~11,500 and ~16,000 for 90 µm (gap=400 nm) and 110 µm (gap=600 nm) radius resonators, respectively.

For both TE and TM polarizations, one determines by fitting experimental results by Eq. 3, the total loss in the ring resonator. This obtained loss corresponds to the propagation loss due to sidewall roughness and to the bend loss. The losses estimated in this way are of about 28 dB/cm (R=90µm) and 16 dB/cm (R=110µm) for both TE and TM polarizations, respectively. These rather high losses are mainly due to the sidewall roughness and few breaks due to stitching problems.

4. Conclusion

We have experimentally demonstrated ring resonator devices based on vertical multiple-slot silicon nitride waveguides for both TE and TM polarizations. High Q-factors have been obtained with such a ring resonator. Indeed, Q-factors as high as 6,100 and 16,000 have been achieved for TE and TM polarizations, respectively. Furthermore, a relatively good agreement between theoretical and experimental group indices is noticeable which indicates that the light is localized inside the slot for TE-polarization and on the silicon nitride rails for TM-polarization.